Manuscript Number:

Title: Disequilibrium melting during crustal anatexis and implications for modelling open magmatic systems.

Short Title: Disequilibrium melting during crustal anatexis

Article Type: Article

Keywords: crustal contamination; anatexis; AFC modelling; Central Andes

Corresponding Author: Claire Louise McLeod

Corresponding Author's Institution: Durham University

First Author: Claire Louise McLeod

Order of Authors: Claire Louise McLeod;Jon Paul Davidson;Geoff Nowell;Shanaka de Silva

Manuscript Region of Origin: BOLIVIA

Abstract: Contamination of ascending mantle-derived magmas by the continental crust was investigated and modelled for a suite of volcanic rocks from the Bolivian Altiplano, Central Andes, using bulk geochemical compositions for mantle-derived and crustal end-members as dictated by traditional approaches. The assumption that the crustal contaminant in these open magmatic systems is a single composition was assessed through in-situ analysis of quenched anatectic melt trapped within its crustal source. Our results show for the first time significant chemical and Sr-isotopic disequilibrium between melt and source over centimetre length scales in a natural system. Sampled glass is rhyolitic and peraluminous in nature and enriched in LREE e.g. Ba, Rb and depleted in HREE e.g. Y and Yb. Analysis of the quenched anatectic melt for its 87Sr/86Sr composition revealed isotopic heterogeneity ranging from 0.7166 to 0.7281. The isotopic disequilibrium between melt and source is understood to reflect the melting of minerals with different Rb/Sr (and therefore 87Sr/86Sr) more quickly than the isotopic composition can diffusively equilibrate between melt and minerals. Our results suggest that the mechanism of crustal anatexis produces contaminating melts which are geochemically heterogeneous both spatially and temporally. This highlights the need for detailed microscopic investigations coupled with petrogenetic modelling in order to develop a more robust characterisation and well constrained quantification of crustal contamination in open magmatic systems.

Suggested Reviewers: Kurt Knesel
Department of Earth Sciences, University of Queensland
k.knesel@uq.edu.au
Has collaborated with J.P. Davidson in the past on studies related to the melting of the crust and is not a collaborator on this project.

Bernardo Cesare
Department of Geoscience, University of Padova

bernardo.cesare@unipd.it
Has an interest in constraining the nature of anatectic melts and has extensively studied partially melted crustal rocks and their relationship to their volcanic hosts in Southeast Spain.

Is not a collaborator on this project.

Tracy Rushmer
Department of Earth and Planetary Sciences, Macquarie University
Tracy.Rushmer@mq.edu.au
Has an interest in characterising partial melting processes and the differentiation between crustal and mantle reservoirs through numerical modelling and experimental studies.

Is not a collaborator on this project.

Anthony Philpotts
Department of Geology and Geophysics, University of Connecticut
Anthony.Philpotts@uconn.edu
Has previously investigated the contamination of ascending magmas by the assimilation of the surrounding wallrock.

Is not a collaborator on this project.

Jon Gamble
School of Biological, Earth and Environment Sciences,, University College Cork
J.Gamble@ucc.ie
Has an interest in the petrogenesis of the continental crust and the geochemical evolution of andesites.

Is not a collaborator on this project.

Opposed Reviewers:

Cover letter

Click here to download Cover letter: McLeod et al_Cover Letter.docx

1   Disequilibrium melting during crustal anatexis and implications for modelling open

2   magmatic systems.

3

4   Claire L. McLeod[1], Jon P. Davidson[1], Geoff M. Nowell[1] and Shanaka L. de Silva[2]

5

6   [1]NCIET, Department of Earth Sciences, Durham University, South Road, Durham, DH1 3LE, UK.

7   [2]Oregon State University, Department of Geosciences, 104 Wilkinson Hall, Corvallis, OR 97331-5506, USA.

8

9

ABSTRACT

11   Contamination of ascending mantle-derived magmas by the continental crust was investigated and modelled

12   for a suite of volcanic rocks from the Bolivian Altiplano, Central Andes, using bulk geochemical compositions

13   for mantle-derived and crustal end-members as dictated by traditional approaches. The assumption that the

14   crustal contaminant in these open magmatic systems is a single composition was assessed through *in-situ*

15   analysis of quenched anatectic melt trapped within its crustal source. Our results show for the first time

16   significant chemical and Sr-isotopic disequilibrium between melt and source over centimetre length scales in a

17   natural system. Sampled glass is rhyolitic and peraluminous in nature and enriched in LREE e.g. Ba, Rb and

18   depleted in HREE e.g. Y and Yb. Analysis of the quenched anatectic melt for its $^{87}Sr/^{86}Sr$ composition revealed

19   isotopic heterogeneity ranging from 0.7166 to 0.7281. The isotopic disequilibrium between melt and source is

20   understood to reflect the melting of minerals with different Rb/Sr (and therefore $^{87}Sr/^{86}Sr$) more quickly than the

21   isotopic composition can diffusively equilibrate between melt and minerals. Our results suggest that the

22   mechanism of crustal anatexis produces contaminating melts which are geochemically heterogeneous both

23   spatially and temporally. This highlights the need for detailed microscopic investigations coupled with

24   petrogenetic modelling in order to develop a more robust characterisation and well constrained quantification of

25   crustal contamination in open magmatic systems.

26

INTRODUCTION

28   During ascent towards the Earth's surface, primary basaltic magma sourced from the mantle has the potential

29   to interact with overlying crustal rocks. This has been recognised since Bowen (1928) argued that assimilation

30   of foreign material into a magma body should be treated as an inevitable consequence of fractional

31   crystallisation, with a positive feedback loop between the extraction of heat due to assimilation and the

32   generation of latent heat of crystallisation as crystallisation is promoted by heat extraction and cooling (e.g.

33   Kuritani et al., 2005). One of the key questions in understanding the origin of igneous rocks at convergent

34   margins (e.g. The Andes) is the fraction and nature of the crustal and mantle reservoirs involved in their

35   petrogenesis. The degree to which mantle and crustal reservoirs have contributed to the geochemical signatures

36   of surface expressions of volcanism at continental arcs is frequently assessed through combined assimilation and

37   fractional crystallisation models (e.g. Taylor, 1980; Spera and Bohrson, 2001). However the nature of potential

38   contaminants is rarely well constrained and the intricacies inherent to crustal anatexis and thus the nature of

39   contaminating crustal melts is left unconsidered.

40   Partial melting redistributes trace elements as a function of their partition coefficients. Isotope ratios however

41   are unaffected by this process and have therefore been implemented as tracers of geochemical reservoirs

42   throughout the Earth. This so-called "fingerprinting" has been widely applied for decades (e.g. Allegre, 1982;

43   Mamani et al., 2010). Sr isotopes are particularly useful at identifying the interaction between crustal and

44   mantle sources as the mantle is relatively nonradiogenic (e.g. $^{87}Sr/^{86}Sr$ of 0.703-0.704, Lucassen et al., 2006)

45   whereas old, high Rb/Sr continental crust is radiogenic (e.g. $^{87}Sr/^{86}Sr$ of 0.735, Taylor, 1980).

46   In order to investigate in detail the geochemical consequences of crustal anatexis and the subsequent

47   implications for modelling contamination processes, the compositions of Central Andean crustal xenoliths and

48   their host Early Pliocene lavas were investigated. These xenoliths provide new constraints to the composition of

49   the Andean continental crust which contaminates ascending mantle-derived magmas. These xenoliths also

50   preserve rare anatectic melts trapped as glass in their protoliths and it is the composition of this glass that offers

51   a unique insight into the behaviour of the crust in open magmatic systems and which challenges our

52   understanding of crustal anatexis and contamination of mantle-derived magmas.

53

SAMPLES

55   Geochemical signatures of crustal xenoliths and their host lavas erupted from monogenetic centres on the

56   Bolivian Altiplano, Central Andes form the basis of this study (Fig. 1a, b). Both centres are small volume

57   comprising of a few flows (~0.04 km^3 at Quillacas, ~0.29 km^3 at Pampas Aullagas), compared with the typical

58   CVZ composite volcanoes of >100 km^3. Sampled lavas from flows at Quillacas (1.42 Ma, 19°S,66°W) and

59   Pampas Aullagas (1.89 Ma, 19°S, 67°W) are andesitic to dacitic and peraluminous (Al$_2$O$_3$ > Na$_2$O+K$_2$O+CaO;

60 15.6-17.1 > 9.4-11.8). They display seriate to porphyritic textures and contain up to 35 vol. % crystals in which

61 phenocrysts, microlites and xenocrysts are present. These lavas preserve a disequilibrium mineral assemblage

62 evidenced by plagioclase displaying sieve textures and oscillatory zoning along with crustal xenocrysts and

63 aggregates of metamorphic minerals. The entrained xenolith lithologies vary from almost pure quartzite to

64 garnet-mica schists with rare granulites and several igneous lithologies including diorites and microgranites.

65 Minerals present include quartz, plagioclase, almandine garnet, biotite, sillimanite ± cordierite ± alkali feldspar

66 ± kyanite ± oxide minerals with accessory epidote, hercynitic spinel, monazite and zircon. Whole rock analyses

67 of sampled lavas clearly indicates crustal contamination has occurred during petrogenesis. This is demonstrated

68 by their extreme Sr-isotopic diversity, ranging from 0.7091-0.7169 (Fig. 1c) and with $^{87}Sr/^{86}Sr$ correlating with

69 indices of differentiation such as SiO_2 (Fig. 1d). The upper limit of this range is one of the most radiogenic

70 compositions to be reported for Central Andean volcanic rocks to date. Lavas erupted at Pampas Aullagas alone

71 record 43% of the observed Sr-isotopic diversity in volcanic rocks from the entire Central Andean region (12%

72 at Quillacas).

73 Identification of extreme isotopic heterogeneity within a single volcanic eruptive unit requires a detailed

74 multi-sampling approach in the field otherwise the complexities of an open magmatic system will be

75 overlooked. The entrained crustal xenoliths display an even greater range of Sr-isotopic compositions ranging

76 from 0.7105 to 0.7368. All sample compositions are provided in the supplementary information.

77

MODELLING CRUSTAL CONTAMINATION

79 Numerous formulations aimed at evaluating and constraining the geochemical evolution in open magmatic

80 systems have been developed over the past few decades e.g. Briqueu and Lancelot, 1979; Taylor, 1980; De

81 Paolo, 1981; Aitcheson and Forrest, 1994; Spera and Borhson, 2001. The objective of these models is to meet

82 the necessity for material mass balance whilst accounting for observed geochemical trends. Although a

83 powerful petrogenetic tool, use of these models is only justifiable if the end member compositions are known

84 i.e. those of the parental mantle-melt and those of the crustal assimilant, and in many studies at least one of

85 those is unknown. Additionally, rates of assimilation to fractional crystallisation (r) and partition coefficients

86 (e.g. D_{Sr}) need to be well constrained. The contaminated nature of the Pampas Aullagas and Quillacas lavas

87 were investigated using the EC(AFC) (Energy Constrained Assimilation and Fractional Crystallisation) model

88 of Spera and Bohrson, (2001). All sampled xenoliths are potential crustal lithologies with which ascending

89 magmas may have interacted. Choosing a suitable parental magma composition is challenging as no true basalts

90   have erupted recently in the Central Andes. Modelling was therefore carried out using a range of oceanic

91   sources along with an older Andean primitive magma represented by a Miocene sill (Chiar Kkollu) from 60km

92   WNW of the field area (Davidson and de Silva, 1992). This basalt (45 wt. % SiO_2 and 9 wt. % MgO) is more

93   primitive than any other lava in this region of the Central Andes. The $^{87}Sr/^{86}Sr$ of the Chiar Kkollu basalt

94   (0.7041) indicates relatively little assimilation of and contamination by the continental crust and its composition

95   may be the closest representative of a parental melt that is currently known for the region. The results are

96   presented in Fig. 1c but offer only a number of possible solutions that model the observed geochemical trends

97   (see supplementary information for model input parameters). Large values of r (>0.6) were required to model

98   the isotopically enriched nature of the lavas. These high values are plausible due to the fusible nature of the

99   meta-pelitic crust and represent 35-50% crustal assimilation which is considerably higher than ~20% as

100 previously estimated for volcanic rocks from the Central Andean arc (Davidson and de Silva, 1992; Aitcheson et

101 al., 1995).

102

103 CRUSTAL ANATEXIS

104 The modelling of crustal contamination assumes that acquisition of a crustal isotopic signature involves 1)

105 mixing of the bulk Sr-isotopic composition of the source crustal rock into an ascending magma and 2) that the

106 composition of this crustal component remains unchanged during concurrent anatexis and contamination.

107 The dominant mechanism of anatectic melt formation in the continental crust is the incongruent melting of

108 hydrous silicates (e.g. biotite) leaving behind a less hydrous restitic assemblage (Stevens et al., 1997). The

109 natural occurrence of preserved anatectic melt within sampled xenoliths offers a rare insight into the primary

110 compositions of potential crustal contaminants as well as constraints on the initial composition of crustal melts

111 produced during orogenesis. .

112 One sample (BC93PAX12) was chosen for an in-depth geochemical study.   Data and details of analytical

113 methods and standards run throughout the course of this study are provided in the supplementary information.

114 The quenched glass is vesiculated, indicating that decompression occurred during and/or after melting (i.e. that

115 melting occurred at depth rather than on eruption). Euhedral hercynitic spinel (<100μm) is present within the

116 melt pools. The presence of this phase has previously been shown to be a common product of the incongruent

117 breakdown of biotite (e.g. Cesare, 2000). All analysed glass is peraluminous in nature (1.77 < A.S.I < 3.00,

118 average 2.08), potassic (up to 5.62 wt. %) and exhibits a restricted range of SiO_2 from 70 to 75 wt. %. The

119 minimum temperature of melting is constrained to >800°C given the coexistence of quartz and hercynitic spinel

120   (Montel et al., 1986). Experiments have shown that crustal melting will typically begin at 780-830°C through

121   the incongruent breakdown of biotite (controlled by Mg number, René et al., 2008) with total biotite breakdown

122   at ~975°C (Stevens et al., 1997). Analysed glass shows enrichment in LREE (Ba, Rb, Fig. 2) and depletion in

123   the HREE that is retained in residual garnet (Fig. 2). The significant Nb depletion recorded in the glass is

124   inferred to represent the stability of anatase, a metastable TiO_2 polymorph which is present as acicular crystals

125   (<200μm). The occurrence of anatase (as opposed to rutile, the more common form of TiO_2) is consistent with

126   the experimental observation that anatase forms under rapid cooling conditions (i.e. quenching) whereas rutile

127   will crystallise under near-equilibrium solidification conditions (Li and Ishigaki, 2002).

128   Analysis of the Sr-isotopic composition of the quenched anatectic melt (Fig. 3a) reveals extreme variability

129   over short length scales and significant isotopic disequilibrium between the melt and its source (Fig. 3b).

130   Sampled glass ranges from 0.7164 to 0.7276 which is more radiogenic than any of the host lavas and associated

131   groundmass glass. The lower end of this range is similar to that of the bulk source xenolith (0.7173). The higher

132   ratios extend beyond any Sr-isotopic compositions recorded by Central Andean volcanic rocks. The crustal

133   signature inferred from the Sr-isotopic composition of volcanic rocks at the surface provides little (if any)

134   information about how it got there nor does it provide any information or constraints on the nature of the

135   contaminant at depth. It is generally accepted that major and trace element abundances of melts from silicate

136   rocks change as melting progresses. Isotope ratios, however, are generally taken to reflect those of the source

137   rock, because it is understood that diffusive equilibrium at the high temperatures of melting is capable of

138   "keeping up" with the melting process. Indeed much of our understanding of isotopically defined mantle

139   reservoirs is predicated on this premise (Hofmann and Hart, 1978). However, if diffusion cannot keep pace with

140   melting then isotopic compositions will vary with the contributions of Sr from the individual phases present

141   within the source (Rushmer and Knesel, 2010). In a magmatic plumbing system where crustal xenoliths are

142   entrained and assimilated in an ascending magma, isotopic disequilibrium melting is likely, and has been

143   documented widely (Al-Rawi and Carmichael, 1967; Pushkar and Stoeser, 1975; Philpotts and Asher, 1993;

144   Hammouda et al., 1994; Hammouda et al., 1996; Knesel and Davidson, 1996; Knesel and Davidson, 1999;

145   Knesel and Davidson, 2002).

146   Old crustal rocks containing phases with variable Rb/Sr will be characterised by Sr isotopic heterogeneity (it

147   is this heterogeneity relative to Rb/Sr which is the basis for Sr isochron dating). Melting will typically begin

148   with preferential breakdown of high Rb/Sr hydrous phases such as biotite, producing an initial melt with a

149   higher $^{87}Sr/^{86}Sr$ than the bulk source. If melting progresses relatively rapidly (so that diffusive equilibration of

150 $^{87}Sr/^{86}Sr$ does not occur), additional phases contribute Sr with different $^{87}Sr/^{86}Sr$ and the composition of the melt

151 weill change as shown schematically in Fig. 4. Feldspar, for instance, has a lower Rb/Sr and will consequently

152 contribute less radiogenic Sr.

153   The Sr isotopic compositions of anatectic melts that contaminate ascending magmas is, therefore, governed by

154 (1) the stoichiometry of melting reactions which controls the changing proportions of phases entering the melt;

155 (2) the rates at which heating and melting occur which define the balance between melt production and the

156 capacity to equilibrate diffusively; (3) the composition of phases consumed, which dictates, in conjunction with

157 (1), the mass balance of Sr in the melt at any given time; (4) the grain size of phases which constrains the length

158 scales of diffusive equilibration; and (5) the timescales of melt segregation (controlled by the permeability of the

159 (molten) source rock and thus grain-scale distribution of the melts, Laporte, 1994). The majority of these

160 factors are left unaccounted for in the current petrogenetic models.

161

162 ## IMPLICATIONS FOR MODELLING NATURAL SYSTEMS

163 The contaminated signatures of volcanic rocks can be reproduced by various model calculations (e.g. Fig. 1c)

164 however it should be noted that these solutions are unlikely to provide a realistic quantification of

165 contamination. In each model, r and D_{Sr} were assumed to remain constant although in reality they may change

166 as differentiation progresses (Roberts and Clemens, 1995). When investigating the petrogenesis of a

167 contaminated volcanic rock suite through AFC modelling the assumption that each erupted unit has interacted

168 with 1) the same crustal lithology and 2) to the same degree, cannot be confidently made. This is demonstrated

169 by the geochemically diverse nature of the crustal xenoliths entrained within lavas at Pampas Aullagas and

170 Quillacas, although the sampled xenoliths are unlikely to represent the full extent of the compositional diversity

171 that exists throughout the 70km thick Central Andean continental crust. It should therefore be unsurprising that

172 erupted volcanic units exhibit highly variable, crustal derived radiogenic Sr-isotopic signatures. A multi-stage,

173 multi-depth plumbing system is likely to exist at depth beneath the centres at Pampas Aullagas and Quillacas

174 where ascending magmas interact with and are contaminated by numerous crustal lithologies as has previously

175 been suggested for larger volcanic edifices (e.g. Davidson and Wilson, 1989).

176 Precise and accurate quantification of the contamination process demands knowledge and understanding of the

177 behaviour of the systems components. The contaminated nature of a suite of volcanic rocks can in principle, be

178 modelled using current petrogenetic models (e.g. Spera and Bohrson, 2001) where the crustal component is

179 constrained by the bulk composition of a sample from the (local) underlying basement and/or a partial melt

180   thereof. Our observations suggest that such approaches should be used with caution and with a thorough

181   understanding of their limitations.

182   There is significant danger in aiming to identify a simple genetic linkage between Sr-isotopic signatures of

183   contaminated volcanic rock suites and sampled (potential) crustal contaminants such as attempted in Fig. 1c and

184   consistently in crustal contamination studies (e.g. Guzmán et al., 2011). As analysis of anatectic melt has

185   shown, significant isotopic disequilibrium exists between product and protolith (Fig. 3b). This has important

186   ramifications for current petrogenetic models which assume a constant isotopic composition for the contaminant

187   (either as a bulk whole rock value or an equilibrium melt thereof). Not only is melting likely to be non modal

188   but anatectic melts will be out of Sr-isotopic equilibrium with their source on the sub-mm scale. Furthermore,

189   the degree of disequilibrium will be heterogeneous throughout the melt as the $^{87}Sr/^{86}Sr$ compositions will be

190   controlled by the relative proportions of the Rb/Sr phases melting at any given point (Fig. 4). The observation

191   that disequilibrium melts can be produced by the incongruent breakdown of variable Rb/Sr phases within the

192   crust supports the explanation regarding the origin of the observed Sr-isotopic disequilibrium between a magma

193   and crystals in an open magmatic system where the composition of the magma from which the crystals are

194   crystallising changes as anatexis proceeds (Duffield and Ruiz, 1998). Further complexity is added when the

195   degree of this heterogeneity through time (i.e. as anatexis proceeds) is considered as a function of the rate of

196   breakdown of these Rb/Sr-bearing phases. A crustal partial melt is not necessarily a simple equilibrium, modal

197   melt, but may be heterogeneous in both space and time (with respect to Sr-isotopes). The process of

198   contamination is complicated further if partial melts from numerous crustal lithologies are incorporated into the

199   same differentiating magma body. These initially highly radiogenic melts are likely to be diluted by continuous

200   melting of less radiogenic phases (Fig. 4). The continuation of anatexis though time acts to dilute the early

201   radiogenically enriched melt phase. Further mixing with a less silica-rich melt (e.g. a recharging mantle-derived

202   magma) may also act to dilute the enriched crustal signature. The observed signature is therefore an average of

203   the entire contamination process and masks the detail and complexities involved in how a crustal signature is

204   acquired.

205   Simplistically, the process of crustal contamination can be viewed as a simple and efficient binary mixing

206   process whereby a new composition is generated as a result of the interaction of two geochemically distinct end

207   members. In reality, the geochemical consequences of crustal anatexis are complex, the process of crustal

208   anatexis is progressive and anatectic melts are not simple partial melts of a source.

209   *In-situ* analysis of anatectic melts associated with their crustal source reveals for the first time the absolute

210   geochemical composition of natural contaminant melts and therefore the potential geochemical signatures that

211   may be derived from them i.e. a relatively high $^{87}Sr/^{86}Sr$ vs. a relatively low $^{87}Sr/^{86}Sr$ contaminant as controlled

212   by the Rb/Sr of the phases incongruently breaking down. This approach highlights the need for a greater

213   appreciation of the complexities inherent to crustal anatexis and the geochemical consequences for modelling

214   the contamination of volcanic rock suites. Hence existing models investigating the petrogenesis of open

215   magmatic systems, combined with microanalysis of potential contaminants will lead to improved quantitative

216   characterisation of the contaminant and the crusts' relative influence on the geochemical signature observed at

217   the surface.

218   Undoubtedly AFC models are useful petrogenetic tools for investigating crustal contributions to mantle-

219   derived magmas however our study highlights the importance of small-scale, microscopic studies in order to

220   improve our understanding of the interaction and transfer between Earth's reservoirs.

221

222

231

232

233 FIGURE CAPTIONS

234

235 Figure 1

236 A. Location map of the Central Volcanic Zone (CVZ; 14°S to 28°S) of the Andean Cordillera, South America.

237 The Northern (NVZ) and Southern (SVZ) Volcanic Zones are also shown (adapted from de Silva, 1989). The

238 area of study is outlined.

239   B. Location of monogenetic mafic centres at Pampas Aullagas and Quillacas on the Bolivian Altiplano.

240   C. Graph showing the Sr-isotopic diversity exhibited by sampled lavas from a single volcanic centre. Modelled

241   EC-AFC curves (after Spera and Bohrson, 2001) for the contaminated nature of the lavas erupted at Pampas

242   Aullagas and Quillacas are also shown. The Miocene basalt of Chiar Kkollu was used as a mantle end-member

243   in all models ($^{87}Sr/^{86}Sr$: 0.7041; Sr: 945ppm) and nine sampled crustal xenoliths were used as potential crustal

244   contaminants ($^{87}Sr/^{86}Sr$ 0.7105-0.7368; Sr: 19-416ppm). The initial path of the EC-AFC curves are flat which

245   reflects the time the crust takes to rise from its initial temperature to its solidus. The end points of each curve

246   depicts the point at which the temperature of the melt (in the magma body) is equal to the equilibration

247   temperature (Spera and Bohrson, 2001). Solutions presented are those which best modelled the data.

248   Compositions of crustal end members and model parameters for each numbered curve (1-13) are provided in the

249   supplementary information.

250   D. Graph showing the increase of $^{87}Sr/^{86}Sr$ with increasing SiO_2 as evidence for assimilation and fractional

251   crystallisation during the petrogenesis of Pampas Aullagas and Quillacas lavas (symbols as in Fig. 1c).

252

253   Figure 2

254   Trace element composition of sampled glass normalised to bulk xenolith BC93PAX12. The pattern reflects the

255   mineralogy of the source whereby elements which are compatible in phases present in the xenoliths and which

256   haven't melted are depleted (e.g. Y in garnet) and those which correspond to biotite melting are enriched (e.g.

257   the LREE). For discussion see text.

258

259   Figure 3

260   A. Sketch depicting quenched glass (black) and unmelted crystalline restite (white) of BC93PAX12. Restite

261   constitutes quartz, biotite, plagioclase, garnet and minor opaque phases. The sampled areas are also highlighted

262   and correspond to the sample numbers in Table 1.

263   B. Sr-isotopic disequilibrium between anatectic melt and bulk source. Glass compositions are age corrected for

264   the Pliocene age of lava eruption.

265

266   Figure 4

267   Hypothetical evolution of the Sr-isotopic composition of an anatectic melt. Crustal anatexis has been shown to

268   commence with biotite melting. During the time which this is the only phase breaking down, the $^{87}Sr/^{86}Sr$

269   composition of the anatectic melt is controlled only by biotite (Bt, controlled by the Rb/Sr). As melting

270   continues, other Rb/Sr bearing phases begin to melt and contribute to the $^{87}Sr/^{86}Sr$ of the anatectic melt e.g.

271   plagioclase (Plg) and alkali feldspar (Ksp). As the proportions of these phases change with time, so too does the

272    $^{87}Sr/^{86}Sr$ of the contaminating crustal melt. Starting compositions of mineral phases are taken from Knesel and

273   Davidson, 2002.

274

275   Table 1

276   Trace element and Sr-isotopic compositions of BC93PAX12 and sampled glass. $^{87}Sr/^{86}Sr_i$ corrected for

277   Pliocene ages of lava eruption. Elemental concentrations are given in ppm unless stated otherwise.

278

279   REFERENCES CITED

280   Aitcheson, S. J., and Forrest, A. H., 1994, Quantification of crustal contamination in open magmatic systems: Journal of
281   Petrology, v. 35, p. 461–488.

282   Aitcheson, S.J., Harmon, R.S., Moorbath, S., Schneider, A., Soler, P., Soria, E.E., Steele, G., Swainbank, I., and Wörner, G.,
283   1995, Pb isotopes define basement domains of the Altiplano, Central Andes: Geology, v. 23, p. 555–558.

284   Allegre, C.J., 1982, Chemical Geodynamics: Tectonophysics, v. 81, p. 109-132.

285   Al-Rawi, Y., and Carmichael, I.S.E., 1967, A note on the natural fusion of Granite: The American Mineralogist, v. 52, p.
286   1806-1814.

287   Briqueu, L., and Lancelot, J. R., 1979, Rb-Sr systematic and crustal contamination models for calc-alkaline igneous rocks,
288   Earth and Planetary Science Letters, v. 43, p. 385-396.

289   Bowen, N.L., 1928, The Evolution of the Igneous Rocks, Dover Publications, New York.

290   Cesare, B., 2000, Incongruent melting of biotite to spinel in a quartz-free restite at el Joyazo (SE Spain): textures and
291   reaction characterisation: Contributions to Mineralogy and Petrology, v. 139, 273-284.

292   Davidson, J.P., and Wilson, I.R., 1989, Evolution of an alkali basalt-trachyte suite from Jebel Marra volcano, Sudan, through
293   assimilation and fractional crystallisation: Earth and Planetary Science Letters, v. 95, p.141-160.

294   Davidson, J.P., and de Silva, S.L., 1992, Volcanic rocks from the Bolivian Altiplano: insights into crustal structure,
295   contamination and magma genesis in the Central Andes: Geology, v. 20, p. 1127–1130.

296   de Silva, S.L., 1989, Altiplano-Puna volcanic complex of the central Andes: Geology, v. 17, p.1102-1106.

297   De Paolo, D.J., 1981, Trace element and isotopic effects of combined wallrock assimilation and fractional crystallization:
298   Earth and Planetary Science Letters, v. 53, p. 189–202.

299   Duffield, W.A., and Ruiz, J., 1998, A model that helps explain Sr-isotope disequilibrium between feldspar phenocrysts and
300   melt in large-volume silicic magma systems: Journal of Volcanology and Geothermal Research, v. 87, p. 7-13.

301 Guzmán S., Petrinovic, I. A., Brod, J. A., Hongn, F. D., Seggiaro, R. E., Montero, C., Carniel, R., Dantas, E. L., and Sudo,
302   M., 2011, Petrology of the Luingo caldera (SE margin of the Puna plateau): a middle Miocene window of the arc-
303   back arc configuration: Journal of Volcanology and Geothermal Research, v. 200, p. 171-191.

304 Hammouda, T., Pichavant, M., and Chaussidon, M., 1994, Mechanisms of isotopic equilibration during partial melting: an
305   experimental test of the behaviour of Sr: Mineralogical Magazine, v. 58A, p. 368-369.

306 Hammouda, T., Pichavant, M., and Chaussidon, M., 1996, Isotopic equilibration during partial melting: an experimental test
307   of the behaviour of Sr: Earth and Planetary Science Letters, v. 144, p. 109-121.

308 Hofmann, A. W., and Hart, S.R., 1978, An assessment of local and regional isotopic equilibrium in the mantle: Earth and
309   Planetary Science Letters, v. 38, p. 44-62.

310 Knesel, K., and Davidson, J. P., 1996, Isotopic disequilibrium during melting of granite and implications for crustal
311   contamination of magmas: Geology, v. 24, p. 243-246.

312 Knesel, K., and Davidson, J. P., 1999, Sr isotope systematics during melt generation by intrusion of basalt into continental
313   crust: Contributions to Mineralogy and Petrology, v. 136, p. 285-295.

314 Knesel, K., and Davidson, J. P., 2002, Insights into Collisional Magmatism from Isotopic Fingerprints of Melting Reactions:
315   Science, v. 296, p. 2206-2208.

316 Kuritani, T., Kitagawa, H., and Nakamura, E., 2005, Assimilation and Fractional Crystallisation controlled by transport
317   process of crustal melt: Implications from an alkali Basalt-Dacite suite from Rushiri volcano, Japan: Journal of
318   Petrology, v. 46, p. 1421-1442.

319 Laporte, D., 1994, Wetting behaviour of partial melts during crustal anatexis: the distribution of hydrous silicic melts in
320   polycrystalline aggregates of quartz: Contributions to Mineralogy and Petrology, v. 116, p. 486-499.

321 Li, Y., and Ishigaki, T., 2002, Thermodynamic analysis of nucleation of anatase and rutile from TiO_2 melt: Journal of
322   Crystal Growth, v. 242, p. 511-516.

323 Lucassen, F., Kramer, W., Bartsch, V., Wilke, H-G., Franz, G., Romer, R. L., and Dulski, P., 2006, Nd, Pb and Sr isotope
324   composition of juvenile magmatism in the Mesozoic large magmatic province of northern Chile (18-27°S):
325   indication for a uniform subarc mantle: Contributions to Mineralogy and Petrology, v. 152, p. 571-589.

326 Mamani, M., Wörner, G., and Sempere, T., 2010, Geochemical variations in igneous rocks of the Central Andean orocline
327   (13°S to 18°S): Tracing crustal thickening and magma generation through time and space: Geological Society of
328   America Bulletin, v. 122, p. 162-182.

329 Montel, J. M., Weber, C., and Pichavant, M., 1986, Biotite-sillimanite-spinel assemblages in high-grade metamorphic rocks:
330   occurrences, chemographic analysis and thermobarometric interest, Bulletin of Mineralogy, v. 109, p. 555-573.

331 Philpotts, A. R., and Asher, P. M., 1993, Wallrock melting and reaction effects along the Higganum diabase dike in
332   Connecticut: contamination of a continental flood basalt feeder: Journal of Petrology, v. 34, p. 1029-1058.

333 Pushkar, P., and Stoeser, D. B., 1975, [87]Sr/[86]Sr ratios in some volcanic rocks and some semifused inclusions of the San
334   Francisco volcanic field: Geology, v. 3, p. 669-671.

335 René, M., Holtz, F., Luo, C, Beermann, O., and Stelling, J., 2008, Biotite stability in peraluminous granitic melts:
336   Compositional dependence and application to the generation of two-mica granites in the South bohemian
337   batholiths (Bohemian Massif, Czech Republic): Lithos, v. 102, p. 538-553.

338 Roberts, M. P and Clemens, J. D., 1995, Feasibility of AFC models for the petrogenesis of calc-alkaline magma series:
339   Contributions to Mineralogy and Petrology, v. 121, p. 139-147.

340 Rushmer, T. and Knesel, K., 2010, Defining Geochemical signatures and timescales of melting processes in the crust: An
341   experimental tale of melt segregation, migration and emplacement. In: Timescales of magmatic processes from
342   core to atmosphere (editors) Dosseto, A., Turner, S. P. and Van Orman, J. A., Wiley-Blackwell.

343 Spera, F. J., and Bohrson, W, A., 2001, Energy-Constrained Open-System Magmatic Processes I: General Model and
344   Energy-Constrained Assimilation and Fractional Crystallization (EC-AFC) Formulation: Journal of Petrology, v.
345   42, p. 999–1018.

346 Stevens, G., Clemens, J. D., and Droop, G. T. R., 1997, Melt production during granulite-facies anatexis: experimental data
347   from "primitive" metasedimentary protoliths: Contributions to Mineralogy and Petrology, v. 128, p. 352-370.

348 Taylor, H. P., 1980, The effects of assimilation of country rocks by magmas on $^{18}O/^{16}O$ and $^{87}Sr/^{86}Sr$ systematic in igneous
349   rock: Earth and Planetary Science Letters, v. 47, p. 243-254.

350
351
352

Table 1
Width: 6.4275cm
Height: 4.8486cm

	whole rock	glass						bulk
	BC93PAX12	1	2	3	4	5	6	
Ba	138.4	357.1	563.6	520.5	1893.0	699.2	146.5	696.7
Rb	27.3	101.8	172.2	178.4	226.6	236.1	84.3	166.7
Th	7.3	2.2	2.2	2.5	4.7	3.8	4.6	3.3
U	1.4	0.8	1.4	1.3	2.0	1.6	2.2	1.5
Nb	17.1	4.0	1.5	1.5	4.0	2.6	4.6	3.0
La	22.4	9.0	10.8	10.7	21.0	15.0	14.9	13.6
Ce	46.0	20.7	30.4	29.9	49.6	37.4	66.8	39.1
Sr	18.5	34.7	56.3	32.3	107.2	37.1	37.2	50.8
Nd	22.8	12.2	15.4	16.3	26.9	21.4	18.0	18.4
Sm	4.7	2.9	3.9	4.0	6.2	5.3	3.5	4.3
Zr	32.8	54.9	112.1	103.8	135.2	119.1	89.7	102.5
Hf	1.1	1.2	2.9	2.6	3.2	2.9	2.2	2.5
Ti	0.3 (wt. %)	0.3	0.3	0.3	0.5	0.4	0.3	0.3
Tb	0.8	0.4	-	0.5	0.9	-	0.5	0.6
Y	30.2	7.6	9.8	11.0	19.6	16.7	21.0	14.3
Yb	5.7	0.3	0.4	0.5	0.7	0.7	1.8	0.7
$^{87}Sr/^{86}Sr$	0.7173	0.7176	0.7209	0.7252	0.7246	0.7281	0.7166	-
$^{87}Sr/^{86}Sr_i$	-	0.7174	0.7207	0.7248	0.7244	0.7276	0.7164	0.7223

Fig. 1
Width: 6.5161cm
Height: 11.7837cm
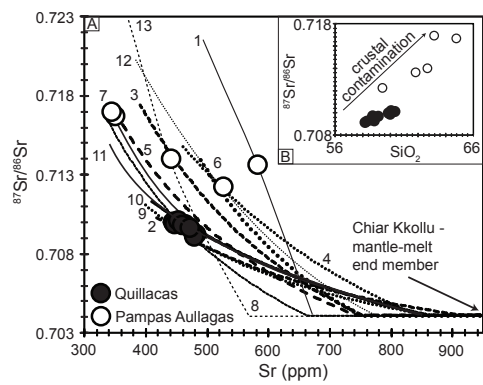
Fig. 2
Width: 6.3796cm
Height: 4.9200cm
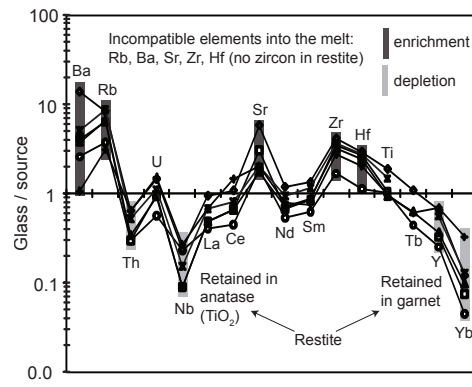
Fig. 3
Width: 6.3975cm
Height: 10.3717cm
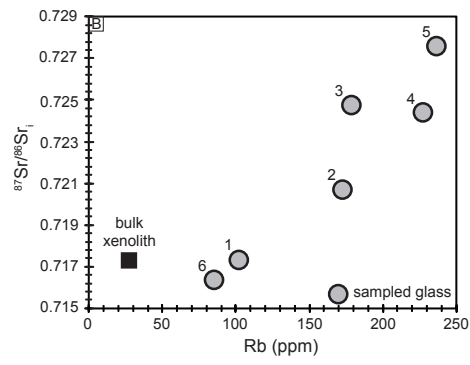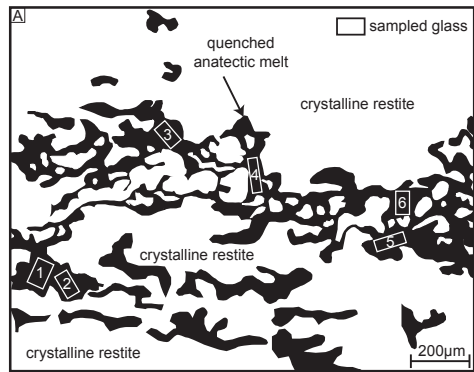
Fig. 4
Width: 6.3975cm
Height: 7.4923cm
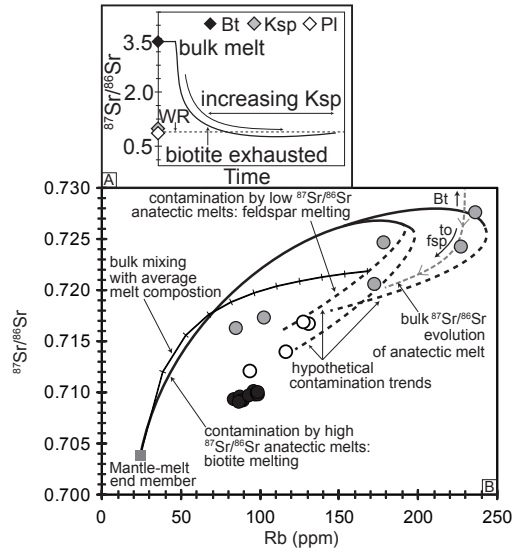
Supplemental file

Click here to download Supplemental file: McLeod et al_Supplementary information_Analytical methods.docx

Supplemental file

Supplemental file

Click here to download Supplemental file: McLeod et al_Supplementary information.xlsx